PCCP

Accepted Manuscript

ROYAL SOCIETY OF CHEMISTRY

www.rsc.org/pccp

Capture of heliophobic atoms by ^{4}He nanodroplets: the case of cesium

Antonio Leal,[1] David Mateo,[2] Alberto Hernando,[3] Martí Pi,[1] and Manuel Barranco[1]

[1] *Departament ECM, Facultat de Física, and IN^{2}UB, Universitat de Barcelona. Diagonal 645, 08028 Barcelona, Spain*

[2] *Department of Chemistry and Biochemistry, California State University at Northridge, 18111 Nordhoff Street, Northridge, California 91330, USA*

[3] *Laboratory of Theoretical Physical Chemistry, Institut des Sciences et Ingénierie Chimiques, Swiss Federal Institute of Technology Lausanne (EPFL), CH-1015 Lausanne, Switzerland*

(Dated: September 8, 2014)

Within Density Functional Theory (DFT), we address the capture of a Cs atom by a superfluid helium nanodroplet using models of different complexity. In the simplest model, the Cs-droplet potential is obtained in two extreme approximations, namely the sudden approximation in which one assumes that the density of the droplet is not relaxed as Cs approaches it, and the adiabatic approximation in which one assumes that it does. Next, a more complex approach in which the collision is described within a time-dependent DFT approach is employed. Depending on the energy and impact parameter of the impinging Cs atom, a rich variety of dynamical phenomena appears that is discussed in some detail.

PACS numbers: 36.40.-c, 67.25.dw, 67.25.dk, 31.15.ee

I. INTRODUCTION

Liquid helium drops formed in free jet expansions of helium gas readily capture atoms and molecules in standard experimental conditions. It was unclear at the beginning whether this was possible or not, since early experiments were interpreted as if ^{4}He droplets were transparent to the dopants.[1] Experiments carried out later on demonstrated that this is not the case, as first shown for Ne atoms captured by ^{4}He drops.[2]

This ability of helium droplets has had a huge impact on the development of the physics and chemistry of helium droplets. Indeed, the isolation of atoms and molecules in ultracold helium droplets made of $10^3 - 10^8$ atoms has allowed to carry out high resolution spectroscopic studies of the dopant and to study chemical reactions at very low temperatures of the order of 0.4 K. Most of the work done in this area has been reviewed in a series of papers, see *e.g.* Refs. 3–11 and references therein.

While many studies on the spectroscopy of impurities attached to helium droplets have been carried out, only a few studies have addressed the capture of dopants by helium droplets. For the present purposes, let us just mention two joint experimental and theoretical works aiming at determining the density profiles of large ^{4}He and ^{3}He droplets from the scattering of Ar and Kr atoms off helium droplets,[12,13] and the microscopic approach to the scattering of ^{3}He and ^{4}He atoms from inhomogeneous quantum liquids of Refs. 14,15 and references therein.

Very recently, the simulation of dynamic processes involving atomic impurities in helium droplets has been undertaken within time-dependent Density Functional Theory (TDDFT). Thus far, TDDFT seems to be the only workable method for the description of real-time process in helium droplets whose size is large enough to allow for a sensible comparison with the current experiments. The method has been applied to the desorption of alkali atoms[16,17] and to the translational dynamics of atoms and cations in the bulk of the droplets.[18–20]

In this work we address the capture of simple atoms by superfluid ^{4}He droplets taking as a study case a heliophobic species, namely a Cs atom impinging on a droplet made of $N = 1000$ helium atoms. It is well known that alkali atoms do not solvate inside ^{4}He droplets but reside in barely bound dimple states at their surface.[21] Studies on Cs are particularly interesting since once captured it is known to stay on the droplet surface even upon photoexcitation.[22] We leave for a forthcoming study the case of a heliophilic species as Xe, for which experiments similar to these of Refs. 12,13 can be carried out.[23]

We first use a rather simple model borrowed from nuclear physics that was employed in the past to describe heavy ion collisions. It allows to obtain the absorption cross section of the Cs atom using as main ingredients the Cs-He pair potential and the droplet density obtained within Density Functional Theory (DFT). Next, a full TDDFT calculation is carried out at several energies and impact parameters. Depending on these physical inputs, we have found that the Cs atom can get stuck to the droplet, orbit around it, bounce back or pass across the droplet. Interestingly, we have found that the capillary waves produced at the droplet surface during the collision process may act as nucleation seeds of quantized ring vortices. This mechanism, similar to that found in Bose-Einstein condensates in confined cold gases,[24] is different from the one by which fast-moving impurities in the superfluid[25] or in the bulk of helium droplets[20] nucleate vortices when the dopant velocity exceeds the Landau critical velocity.

This paper is organized as follows. In Sec. II we describe a simple method to calculate the absorption cross section and the results obtained in two extreme approximations. In Sec. III we briefly present the method we use

to describe the Cs-droplet collision within the TDDFT approach as well as the results obtained with it. Finally, a summary is presented in Sec IV.

II. A SIMPLE MODEL FOR IMPURITY STICKING

Inspired in the nucleon-nucleus collision phenomenology, a liquid drop plus optical model was used in the past to address elastic, inelastic and absorptive scattering of ^{4}He atoms from ^{4}He droplets.[26] It is possible to obtain the cross section for the capture of a Cs atom by a helium droplet using a well-established phenomenological model also borrowed from nuclear physics.[27] The cross section for the capture is written as[28]

$$\sigma(E) = \frac{\pi}{\kappa^2} \sum_{\ell=0}^{\infty} (2\ell+1) T_\ell \tag{1}$$

with

$$\kappa = \sqrt{\frac{2\mu E}{\hbar^2}} \ , \tag{2}$$

where μ is the reduced mass of the system and E is the available energy in the center-of-mass framework. T_ℓ is the ℓ-th transmission coefficient leading to the capture of Cs in the ℓth-channel, where ℓ is the droplet-impurity relative angular momentum in $\hbar$ units in that channel.

For a large helium droplet *at rest*, since its mass is much larger than the Cs atom mass, it would be justified to identify the center-of-mass of the droplet+impurity framework, where collision theory is formulated,[29] with the laboratory framework, taking for μ the mass of Cs and for the center-of-mass of the system that of the helium droplet, identifying E with the kinetic energy of Cs in the laboratory and ℓ with the angular momentum of the impinging impurity with respect to the center-of-mass of the droplet. In actual experiments, neither the droplet nor the impurity are at rest. Rather, the impurity atoms in a secondary beam cross the droplet beam at some angle.[12,13] Unless explicitly stated, all the results presented in this work are discussed in the framework in which the helium droplet is at rest before the collision. In this frame, the center-of-mass sensibly coincides with that of the droplet, and the relative angular momentum with the angular momentum of the Cs atom with respect to the center-of-mass of the droplet. Expressing cross sections and other physical observables in one frame or another involves kinematic transformations that depend on the state of motion of the target (droplet) and projectile (Cs)[29] in a particular experiment but are not so relevant for the present purposes.

Provided that the reduced de Broglie wave length of cesium $\lambda\!\!\!^{-}_{\rm Cs} \equiv 1/\kappa \ll$ dimension of the droplet, the system behaves classically and T_ℓ abruptly goes from 0 to 1 in a ℓ-range small compared with the range of ℓ values leading to capture. We have checked that this is the case for a $N = 1000$ atoms droplet and a typical velocity of 100 m/s. We can thus take $T_\ell = 1$ up to a critical ℓ value ℓ_{cr} (sharp cut-off approximation). Hence,

$$\sigma(E) = \frac{\pi}{\kappa^2} \sum_{\ell=0}^{\ell_{cr}} (2\ell+1) = \frac{\pi}{\kappa^2} (\ell_{cr}+1)^2 \tag{3}$$

In order to determine ℓ_{cr}, we proceed as follows. Firstly, we obtain the Cs-droplet interaction potential as a function of the distance $\mathbf{R}$ between the center of mass of the droplet and the location of the Cs atom. We have two possibilities: either we relax the helium density $\rho(\mathbf{r})$ for given $\mathbf{R}$ (adiabatic approximation), of we keep $\rho(\mathbf{r})$ spherical (sudden approximation). In both cases, the total interaction potential is obtained by adding to V(R) the centrifugal term, getting for a given ℓ value the effective potential

$$V_\ell(R) = V(R) + \frac{\ell(\ell+1)\hbar^2}{2\mu R^2} \tag{4}$$

As $V(R)$ has an attractive part and $\ell(\ell+1)\hbar^2/2\mu R^2$ is repulsive and dominant at large distances, $V_\ell(R)$ has some structure. For the cases of interest here, it displays a local minimum ("pocket") followed by a local maximum, *i.e.*, there is a barrier hindering the capture unless the available energy (kinetic energy of Cs) is high enough to overcome it. If it is too large, processes as disintegration of the droplet or Cs passing across it may happen. We discard these possibilities.

After the barrier is overcome, it is assumed that dissipation comes very efficiently into play and the Cs atom is drawn to the minimum of the potential being trapped. For a given E, the largest ℓ leading to the capture of Cs defines ℓ_{cr}. For $V_{\ell_{cr}}$ the pocket and the barrier collapse and their energy is equal to the impinging Cs energy E. Within this model, the existence of the pocket is instrumental for the capture.

A. Sudden approximation

In terms of the Cs-He pair potential V_X[30] and the spherically symmetric equilibrium density of the pure ^{4}He$_{1000}$ droplet obtained using the Orsay-Trento (OT) functional[31] we have

$$V(\mathrm{R}) = \int d\mathbf{r} \rho(\mathbf{r}) V_X(|\mathbf{r}-\mathbf{R}|) \ . \tag{5}$$

Figure 1 shows the sudden potential V_ℓ for several ℓ values. Notice the appearance of the pocket and barrier structures up to $\ell = 300$. The figure shows that $\ell_{cr} = 300$

for Cs approaching $^4He_{1000}$ at $v_{Cs} = 100$ m/s (corresponding to a kinetic energy of 80 K) and impact parameter $b_{cr} = 14.5$ Å; we recall that the impact parameter b is defined as $\ell\,\hbar = m_{Cs}\,v_{Cs}\,b$ and hence $\ell_{cr}\,\hbar = m_{Cs}\,v_{Cs}\,b_{cr}$. The capture cross section is $\sigma = 665$ Å^2. The cross sections calculated in Ref. 12 for Ar and Kr atoms are about three times larger and include the elastic contribution to it. If $\ell_{cr} \gg 1$, Eq. (3) and the above definition yield $\sigma = \pi\, b_{cr}^2$. Since the sharp density radius of the droplet $R_0 = r_0 N^{1/3}$ (with $r_0 = 2.22$ Å) is 22.2 Å for $N = 1000$, it appears that the sticking cross section is similar to the geometrical cross section.

B. Adiabatic approximation

In this case one has to minimize the energy of the Cs@$^4He_{1000}$ complex keeping the Cs atom a distance R apart from the center of mass of the droplet.[17] Then

$$V(\mathrm{R}) = E[\mathrm{Cs@}^4\mathrm{He}_{1000}(R)] - E[^4\mathrm{He}_{1000}] \ , \qquad (6)$$

where $E[\mathrm{Cs@}^4\mathrm{He}_{1000}(R)]$ is the energy of the Cs-droplet complex and $E[^4\mathrm{He}_{1000}]$ is the energy of the pure droplet, both calculated within DFT.

Figure 2 shows the adiabatic potential V_ℓ for several ℓ values. The potential for $\ell = 0$ is consistent with that found in a similar calculation by Callegari and Ancilotto,[32] which displays a minimum of about 14 K at a distance of ~ 33.5 Å (see Fig. 8 of this reference), but for a $N = 2000$ droplet. For this reason, the minimum of their potential is deeper and located at a larger distance.

We have found that $\ell_{cr} = 375$ for Cs approaching $^4He_{1000}$ at 100 m/s and impact parameter $b_{cr} = 17.9$ Å. The capture cross section is $\sigma = 1012$ Å^2. As in the adiabatic approximation one relaxes the helium density, the critical angular momentum and cross sections are larger than in the sudden approximation since part of the available energy and angular momentum have been deposited into the droplet before the capture of the impurity. Notice that the value of b_{cr} is similar to the radius of the droplet. This means that if dissipation acts efficiently transferring the incoming energy into excited modes of the droplet and/or evaporation of helium atoms, the capture cross section is similar to the geometric cross section of the droplet.

III. REAL-TIME DYNAMICS WITHIN TDDFT

The dynamics is triggered by giving to the Cs atom some kinetic energy and angular momentum or, equivalently, some velocity v_{Cs} and impact parameter b (in the framework where the droplet is at rest before the collision). The Cs atom has been initially placed 32 Å away of the center-of-mass of the droplet. Within TDDFT, we represent the He droplet by a complex effective wave function $\Psi_{He}(\mathbf{r},t)$ such that $\rho(\mathbf{r},t) = |\Psi_{He}(\mathbf{r},t)|^2$. The Cs atom is treated classically as its mass is much larger than the He atom mass. Hence, its position $\mathbf{r}_{Cs}(t)$ obeys the Newton equation. We have[17]

$$\begin{aligned} i\hbar\frac{\partial}{\partial t}\Psi_{He} &= \left[-\frac{\hbar^2}{2m_{He}}\nabla^2 + \frac{\delta\mathcal{E}_{He}}{\delta\rho(\mathbf{r})} + V_X(|\mathbf{r}-\mathbf{r}_{Cs}|)\right]\Psi_{He} \\ m_{Cs}\ddot{\mathbf{r}}_{Cs} &= -\nabla_{\mathbf{r}_{Cs}}\left[\int d\mathbf{r}\rho(\mathbf{r})V_X(|\mathbf{r}-\mathbf{r}_{Cs}|)\right] \\ &= -\int d\mathbf{r}[\nabla\rho(\mathbf{r})]V_X(|\mathbf{r}-\mathbf{r}_{Cs}|)\ , \qquad (7) \end{aligned}$$

where $\mathcal{E}_{He}$ is the OT potential energy density per unit volume. Eqs. (7) have been discretized in cartesian coordinates using a spatial grid of 0.4 Å. The spatial derivatives have been calculated with 13-point formulas. Fast-Fourier techniques have been employed to efficiently calculate the energy density and mean-field potential.[33] The dynamics has been followed using a predictor-corrector method[34] fed by a few time steps obtained by a fourth-order Runge-Kutta algorithm. A time step of 1 fs has been used. This time step can be compared with the period τ_λ of surface λ-mode oscillations of a spherical helium droplet of radius R_0, atom density ρ_0 and surface tension σ, whose energy within the liquid drop model are given by[35]

$$E_\lambda = \frac{h}{\tau_\lambda} = \sqrt{\frac{\hbar^2\,\gamma}{\rho_0\,m_{He}\,R_0^3}\lambda\,(\lambda-1)\,(\lambda+2)} \qquad (8)$$

Taking the values corresponding to ^{4}He $\rho_0 = 0.0218$ Å^{-3}, $\gamma = 0.274$ K Å^{-2} and $\hbar^2/m_{He} = 12.12$ K Å^2 one obtains for the quadruple mode of the $N = 1000$ droplet $E_2 = 0.33$ K and hence $\tau_2 = 1.45$ ps. Thus, our time resolution is expected to cover the relevant aspects of the dynamics.

Even within TDDFT, the calculations are very time consuming. On the one hand, the mean field potentials in Eq. (7) are cumbersome to obtain in the case of helium as compared to those entering the much simpler time-dependent Gross-Pitaevskii equation for cold gases.[24] On the other hand, the calculation box must be large enough to accommodate a large droplet. We have used a three dimensional grid made of $180 \times 180 \times 256$ points. For these reasons, rather than presenting systematic results we have limited ourselves to the discussion of several cases relevant for the physics of impurity capture.

A. Head-on collisions

We have carried out simulations for Cs atoms impinging on the $^4He_{1000}$ droplet at $v_{Cs} = 50$, 75, 100, and 200 m/s and impact parameter $b = 0$. As the electronic supplementary information (ESI) shows,[36] the Cs atom is captured at 50 m/s, barely escapes the droplet at 75 m/s, bounces back at 100 m/s, and pierces through the

droplet at 200 m/s. Notice that at a given velocity, peripheral $b \neq 0$ collisions cannot lead to Cs capture if the corresponding head-on collision does not, as energy is less efficiently dispersed into the droplet for the former than for the later.

The energy has to be very efficiently transferred into the droplet for the impurity to stick to its surface. The simulation at 100 m/s shown in Fig. 3, corresponding to a Cs kinetic energy $E_{kin} = 80$ K, is very illustrative of the difficulties inherent to the simulation of the capture process. The Cs atom bounces back at ~ 10 m/s ($E_{kin} = 0.8$ K), indicating that 99% of the available energy in the entrance channel has been transferred to excited modes of the droplet as ripplons, phonons, maxons, rotons, vortices, ... (we have not detected any appreciable atom evaporation off the calculation cell). For Cs to be captured, the droplet has to dissipate that energy plus the binding energy of the impurity to the droplet. Using the OT functional, we have calculated this binding, $E[^4\mathrm{He}_{1000}] - E[\mathrm{Cs@}^4\mathrm{He}_{1000}] = 10.5$ K. A value of 13.5 K was found by Ancilotto *et al.* for a planar helium surface using a different functional and Xe-He interaction.[37] A larger value should be expected for the planar geometry due to curvature effects, see. *e.g.* Ref. 38.

The simulation at 75 m/s shown in Fig. 4 illustrates that dynamic effects may dramatically alter the potential well that binds the impurity to the droplet surface: a local deformation of the surface around the Cs atom "kicks it out" when the impurity seemed apparently stuck to the droplet. This limiting case defines the velocity at which Cs is captured, which is some 4-5 times smaller than typical thermal velocities in the pickup chamber. As the OT functional properly describes the elementary excitations of liquid helium,[39] one possible source for this disagreement is that the TDDFT approach does not yield enough atom evaporation at low energies. We want to mention however, that TDDFT may yield appreciable evaporation if the energy deposited is large.

The simulation at 200 m/s in Fig. 5 shows that Cs goes across the helium droplet without being captured. It also displays the appearance of a ring vortex nucleated at surface region of the droplet opposite to the collision point. Calculation of the circulation around the vortex core yields a value of unity in units of h/m_{He}, indicating that this ring vortex is quantized, and so are the others discussed in this work.

As it can be seen,[36] the vortex nucleates from the collapse of a surface perturbation created at the point of impact that has traveled from it as a "circular" tidal wave. The vortex energy E_{ring} can be estimated by the expression[25]

$$E_{ring} = \frac{2\pi^2\hbar^2}{m_{\mathrm{He}}}\rho_0 R\left(\ln\frac{8R}{a} - 1.615\right) \quad , \qquad (9)$$

with a the vortex core radius, R the ring radius and ρ_0 the helium number density at large distance. Taking the values for the present system, $a = 1.0$ Å, $R = 3.9$ Å and $\rho_0 = 0.0218\text{Å}^{-3}$ corresponding to the number density of a pure helium droplet, we obtain an energy of ~ 17.7 K. We want to indicate that the values of some variables discussed in this section have been obtained from an analysis as accurate as possible of the ESI that is in a graphic format. For this reason, they cannot be but estimates.

After nucleating at the droplet surface, the ring vortex penetrates into the droplet with a self-induced velocity[25]

$$v_{ring} = \frac{\hbar}{2m_{\mathrm{He}}R}\left(\ln\frac{8R}{a} - 0.615\right) \quad . \qquad (10)$$

Using the previous values, we find $v_{ring} \sim 37.6$ m/s. One should have in mind that Eqs. (9) and (10) are only valid in the limit of $R \gg a$. Fig. 6 displays the ring vortex approaching the Cs bubble a few picosecond before they collide and the vortex is annihilated. Superimposed on the helium density displayed in this figure are the circulation lines. These clearly reveal a circular flow field around the vortex.

The Cs atom eventually detaches from the droplet with a velocity $v_{\mathrm{Cs}} \sim 64.7$ m/s, having thus deposited into the droplet about a 90 % of the energy available in the entrance channel (320 K). Notice that the angular momentum involved in the process is zero; we recall that, at variance with a linear vortex or a vortex loop,[25] a ring vortex carries no net angular momentum.

A ring vortex is also nucleated in the Cs-droplet collision at 100 m/s. In this case, it is immediately washed out by the incoming density waves.[36] For smaller velocities (50 m/s and 75 m/s), the velocity of the impurity in the droplet does not exceed the Landau critical velocity and vortices are not nucleated. We notice that the simulation at 50 m/s shows the capture of the Cs atom by the droplet.[36]

B. Peripheral collisions and angular momentum deposition

We have carried out a simulation at $v_{\mathrm{Cs}} = 100$ m/s with an impact parameter $b = 11$ Å, *i.e.*, about half the value of the sharp density radius of the droplet.[36] In this case, some angular momentum is also deposited into the droplet. After the collision, the Cs atom emerges at $v_{\mathrm{Cs}} \sim 15.3$ m/s, having transferred to the droplet a 98 % of the available energy. The angular momentum in the entrance channel is $L = m_{\mathrm{Cs}}\, v_{\mathrm{Cs}}\, b = 230\hbar$. Part of it is taken away by the outgoing Cs atom ($\sim 114\hbar$); the angular momentum deposited into excited modes of the droplet is $\sim 105\hbar$, and the remaining $11\hbar$ are taken by the droplet as a whole in the recoil of its center-of-mass, some 6.6 Å during the 225 ps we have followed this collision (average velocity ~ 3 m/s).

How angular momentum can be deposited into a helium droplet that cannot be set into rotation because it is superfluid and its velocity field is irrotational is an interesting issue.[24,40,41] One possibility is by nucleating vor-

tex lines that start and end at the droplet surface.[42–44] In particular, a linear vortex along the diameter of a droplet with N atoms carries $N\hbar$ angular momentum. If there are no vortices in the droplet, the superfluid droplet may store angular momentum into surface waves, while the flow inside the droplet is still irrotational.

Figure 7 and the electronic supplementary information corresponding to the $v_{\rm Cs} = 50$ m/s, $b = 11$ Å collision seem to display a dimple at the droplet surface that "rigidly" rotates as the droplet does, dragging along the Cs atom. This is quite not so: the dimple travels on the droplet surface along with the impurity, without this meaning that the bulk of the droplet rotates, which is prevented by the irrotational character of the superfluid flow. We have calculated the flow pattern at $t = 385$ ps and show it in Fig. 8. It can be seen that the flow pattern in the laboratory fixed framework corresponds to an irrotational fluid instead of a rigid rotation. Hence, while the superfluid helium droplet may appear to an observer in the laboratory as a deformed droplet rigidly rotating, Fig. 8 clearly shows that it does not. Similar patterns can be found *e.g.* in Refs. 40,41. The angular momentum available in the collision is thus deposited into capillary waves traveling on the droplet surface, partly is taken away by promptly emitted helium atoms, and some remains in the impurity.

Decreasing the impact parameter to $b = 9$ Å, the Cs atom orbits around the core of the droplet.[36] This is one of the possibilities for the scattering of a particle by an attractive potential. Fig. 9 displays the collision at $v_{\rm Cs} = 50$ m/s and impact parameter $b = 9$ Å. Notice that in this case the dynamics has been followed for more than 1.3 ns. The results at 50 m/s indicate that the critical impact parameter at this energy is $b_{cr} \sim 10$ Å and hence $\ell_{cr} = 94$. Eq. (3) yields a cross section of 260 Å^2 for the capture of Cs by this droplet at 50 m/s.

IV. SUMMARY AND OUTLOOK

We have studied the collision of a heliophobic Cs impurity with a $^4{\rm He}_{1000}$ droplet within TDDFT, obtaining a rich phenomenology depending on the impinging energy and impact parameter of the Cs atom.

For a head-on collision at the higher energy here addressed (Cs at 200 m/s) the droplet turns out to be "transparent" to the impurity in the sense that it goes across the droplet after having deposited into it a large part of its kinetic energy. Experimental evidence for the transmission of ^{3}He atoms through superfluid ^{4}He droplets was presented in Ref. 45, although other possibilities to interpret the experiment were discussed in the same reference. As the kinetic energy decreases one observes that the impurity is first reflected (impinging velocities of 100 m/s and 75 m/s) and eventually it is captured by the droplet (impinging velocity of 50 m/s).

We have also addressed peripheral collisions, in which case not only energy but also angular momentum is deposited into the droplet. This has allowed us to visualize the irrotational flow of the superfluid helium inside the droplet and the nucleation of ring vortices from the large deformations produced at the droplet surface that also appear in head-on collisions. At low energies and small impact parameters the impurity is captured by the droplet, sometimes leading to its orbiting around the center-of-mass of the droplet.

It should be noted that while the theoretical phenomenology is consistent with the experimental findings, it appears at lower energies. Current experiments on Cs atoms involve velocities in the pickup chamber of the order of 400 m/s, for which our simulations yield droplet transparency. This discrepancy might hint that doping droplets with heliophobic dopants require of multiple collisions with droplets in the beam before they lose enough energy to be captured by one of them. This could be discerned by studying how the signal coming from single dopants attached to droplets scales with dopant density. It might also be a consequence of using in the simulations a mean field approach as TDDFT that, while it incorporates helium atom ejection as a possible energy dissipation mechanism,[20] it likely underestimates it, hindering the sticking of the weakly interacting heliophobic impurity. We recall that, according to our analysis of the Cs-droplet head-on collision at 100 m/s, the prompt emission of just two helium atoms would take away enough energy allowing for Cs to stick to the droplet surface. The interested reader might also look at Ref. 46 for a comparison between the TDDFT and classical Molecular Dynamics methods applied to the collision of a pure $^4{\rm He}_{300}$ droplet at 200 m/s with a TiO_2 surface. It can be seen that within TDDFT, the droplet collision yields the ejection of helium atoms ("evaporation") and the spreading of most of the original droplet on the TiO_2 surface, that is wet by helium as most materials at temperatures low enough –the calculation was performed at zero temperature. The classical Molecular Dynamics approach yields the opposite behavior, with the splashing of the droplet out of the surface upon impact.

Ascertaining how well the present formalism works for a simple heliophilic impurity as xenon would help seize the limitations of the TDDFT simulations in this respect before undertaking any substantial improvement of the approach that might incorporate in a workable way efficient helium atom evaporation. We plan to address this issue in a forthcoming paper.

Acknowledgments

We would like to thank Frank Stienkemeier and Marcel Mudrich for useful discussions. This work has been performed under Grants No. FIS2011-28617-C02-01 from DGI, Spain (FEDER) and 2009SGR1289 from Generalitat de Catalunya. AL has been supported by the ME (Spain) FPI program, Grant No. BES-2012-057439.

[1] J. Gspann, Physica B+C **108**, 1309 (1981).
[2] A. Scheidemann, J.P. Toennies, and J.A. Northby, Phys. Rev. Lett **64**, 1899 (1990).
[3] J.P. Toennies and A.F. Vilesov, Angew. Chem. Phys. **43**, 2622 (2004).
[4] M. Barranco, R. Guardiola, S. Hernández, R. Mayol, J. Navarro, and M. Pi, J. Low Temp. Phys. **142**, 1 (2006).
[5] K. Szalewicz, Int. Rev. Phys. Chem. **27**, 273 (2006).
[6] F. Stienkemeier and K.K. Lehmann, J. Phys. B **39**, R127 (2006).
[7] M.Y. Choi, G.E. Douberly, T.M. Falconer, W.K. Lewis, C.M. Lindsay, J.M. Merritt, P.L. Stiles, and R.E. Miller, Int. Rev. Phys. Chem. **25**, 15 (2006).
[8] J. Tiggesbäumker and F. Stienkemeier, Phys. Chem. Chem. Phys. **9**, 4748 (2007).
[9] A. Slenczka and J.P. Toennies, in *Low Temperatures and Cold Molecules*, p. 345. W.M. Smith editor (World Sci., Singapore 2008).
[10] C. Callegari and W. E. Ernst, in *Handbook of High Resolution Spectroscopy*, vol 3 p. 1551 (Whiley, New York 2011).
[11] M. Mudrich and F. Stienkemeier, arXiv:1406.4697v1 [physics-atm-clus] 18 Jun 2014, to be published in the Int. Rev. Phys. Chem.
[12] J. Harms, J.P. Toennies, and F. Dalfovo, Phys. Rev. B **58**, 3341 (1998).
[13] J. Harms, J.P. Toennies, M. Barranco, and M. Pi, Phys. Rev. B **63**, 184513 (2001).
[14] E. Krotscheck and R.E. Zillich, Eur. Phys. J. D **43**, 113 (2007).
[15] E. Krotscheck and R.E. Zillich, Phys. Rev. B **77**, 094507 (2008).
[16] A. Hernando, M. Barranco, M. Pi, E. Loginov, M. Langlet, and M. Drabbels, Phys. Chem. Chem. Phys. **14**, 3996 (2012).
[17] J. von Vangerow, A. Sieg, O. John, A. Leal, D. Mateo, M. Barranco, A. Hernando, M. Pi, F. Stienkemeier, and M. Mudrich, dx.doi.org/10.1021/jp503308w.
[18] D. Mateo, A. Hernando, M. Barranco, E. Loginov, M. Drabbels, and M. Pi, Phys. Chem. Chem. Phys. **15**, 18388 (2013).
[19] N.B. Brauer, S. Smolarek, E. Loginov, D. Mateo, A. Hernando, M. Pi, M. Barranco, W.J. Buma, and M. Drabbels, Phys. Rev. Lett. **111**, 153002 (2013).
[20] D. Mateo, A. Leal, A. Hernando, M. Barranco, M. Pi, F. Cargnoni, M. Mella, X. Zhang, and M. Drabbels, J. Chem. Phys. **140**, 131101 (2014).
[21] O. Bünermann, G. Droppelmann, A. Hernando, R. Mayol, and F. Stienkemeier, J. Phys. Chem. A **111**, 12684 (2007).
[22] M. Theisen, F. Lackner, and W.E. Ernst, J. Chem. Phys. **135**, 074306 (2011).
[23] M. Lewerenz, B. Schilling, and J.P. Toennies, J. Chem. Phys. **102**, 8191 (1995).
[24] L. Pitaevskii and S. Stringari, *Bose-Einstein Condensation*, International Series of Monographs on Physics **116** (Clarendon Press, Oxford 2003).
[25] R.J. Donnelly, *Quantized vortices in helium II*, Cambridge Studies in low Temp. Phys., vol 3 (1991).
[26] D. Eichenauer, A. Scheidemann, and J.P. Toennies, Z. Phys. D **8** 295 (1988).
[27] C. Ngô, Progress in Particle and Nuclear Physics **16**, 139 (1986).
[28] S. Gasiorowicz, *Quantum Physics*, 3rd. ed. (John Wiley & Sons, New York 2003).
[29] C.J. Joachain, *Quantum Collision Theory*, (North-Holland, Amsterdam 1975).
[30] S.H. Patil, J. Chem. Phys. **94**, 8089 (1991).
[31] F. Dalfovo, A. Lastri, L. Pricaupenko, S. Stringari, and J. Treiner, Phys. Rev. B **52**, 1193 (1995).
[32] C. Callegari and F. Ancilotto, J. Phys. Chem. A **115**, 6789 (2011).
[33] M. Frigo and S.G. Johnson, Proc. IEEE **93**, 216 (2005).
[34] A. Ralston and H. S. Wilf, *Mathematical methods for digital computers* (John Wiley and Sons, New York, 1960).
[35] M. Casas and S. Stringari, J. Low Temp. Phys. **79**, 135 (1990).
[36] See the electronic supplementary information for the continuous movies corresponding to the collisions.
[37] F. Ancilotto, E. Cheng, M.W. Cole, and F. Toigo, Z. Phys. B **98**, 323 (1995).
[38] F. Stienkemeier, O. Bünermann, R. Mayol, F. Ancilotto, M. Barranco, and M. Pi, Phys. Rev. B **70**, 214509 (2004).
[39] We have neglected the backflow term in the OT functional because it is ill-behaved at low densities.[31] As a consequence, the Landau velocity is overestimated meaning that rotons may be excited in the superfluid but when impurities move at higher velocities.[18]
[40] A. Bohr and B.R. Mottelson, *Nuclear Structure*, vol. II, Appendix 6A (W.A. Benjamin, Reading, Ma. USA, 1975).
[41] G.M. Seidel and H.J. Maris, Physica B **194-196**, 577 (1994).
[42] G.H. Bauer, R.J. Donnelly, and W.F. Vinen, J. Low Temp. Phys. **98**, 47 (1995).
[43] F. Dalfovo, R. Mayol, M. Pi, and M. Barranco, Phys. Rev. Lett. **85**, 1028 (2000).
[44] K.K. Lehmann and R. Schmied, Phys. Rev. B **68**, 224520 (2003).
[45] J. Harms and J.P. Toennies, Phys. Rev. Lett. **83**, 344 (1999).
[46] N.F. Aguirre, D. Mateo, A.O. Mitrushchenkov. M. Pi, and M.P. de Lara-Castells, J. Chem. Phys. **136**, 124703 (2012).

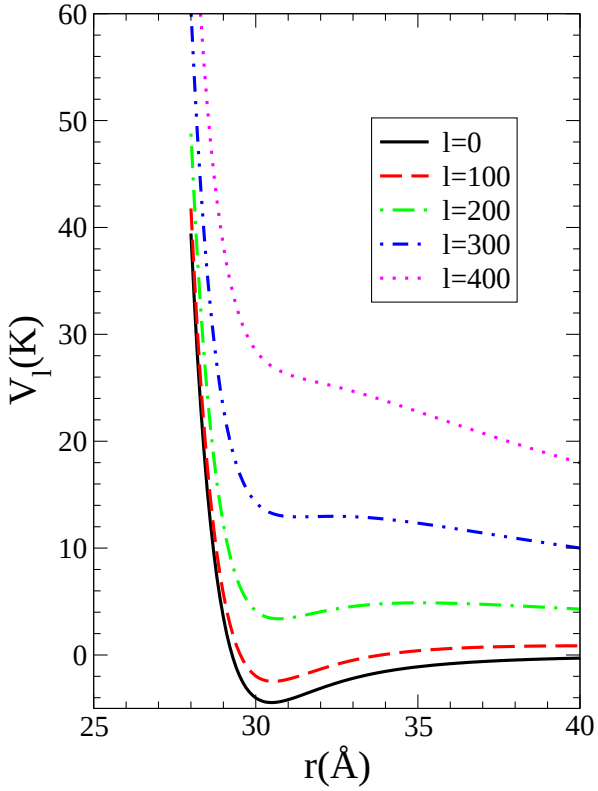

FIG. 1: Sudden potential $V_\ell(r)$ (K) as a function of r (Å) for several ℓ values.

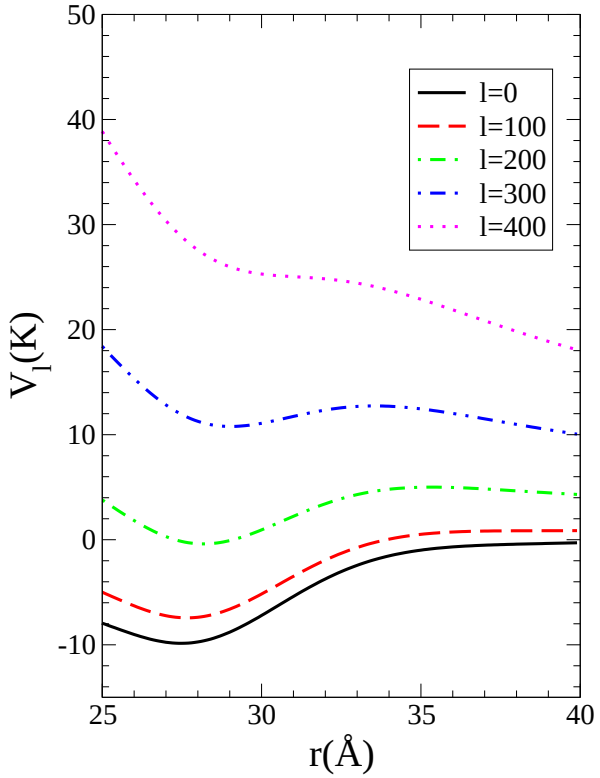

FIG. 2: Adiabatic potential $V_\ell(r)$ (K) as a function of r (Å) for several ℓ values.

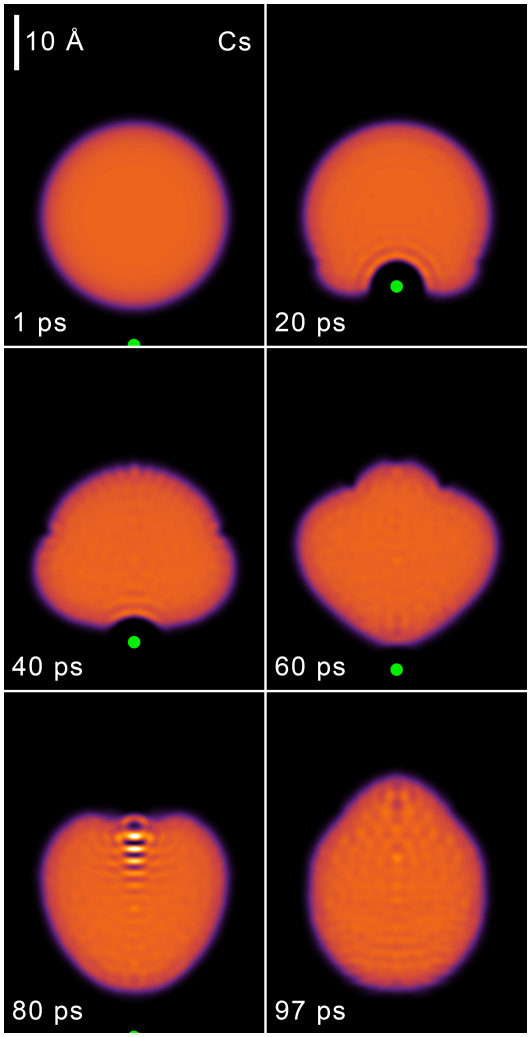

FIG. 3: Dynamic evolution of Cs (big dot) approaching from below the $N = 1000$ helium droplet at $v_{\mathrm{Cs}} = 100$ m/s and $b = 0$, eventually bouncing back. The corresponding time is indicated in each frame.

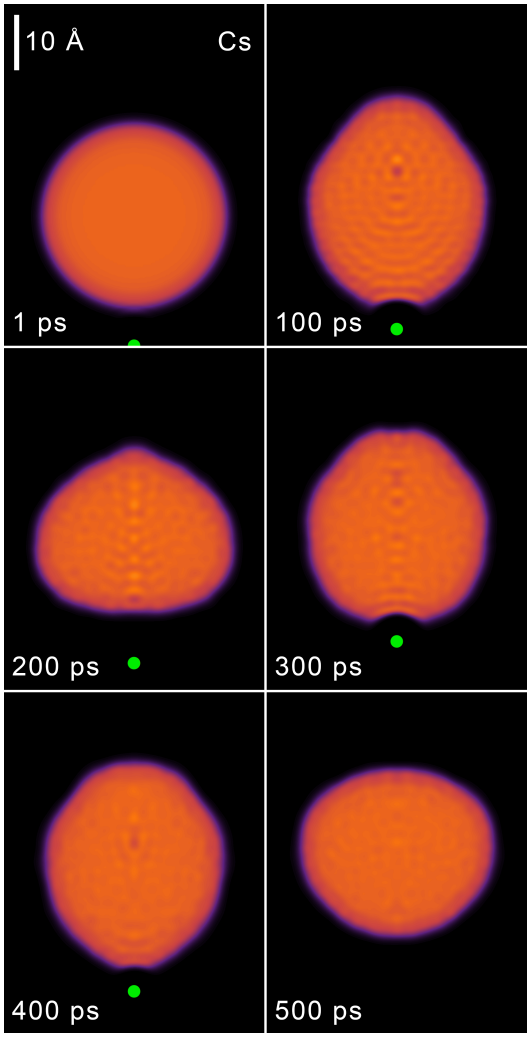

FIG. 4: Dynamic evolution of Cs (big dot) approaching from below the $N = 1000$ helium droplet at $v_{Cs} = 75$ m/s and $b = 0$, nearly captured by it. The corresponding time is indicated in each frame.

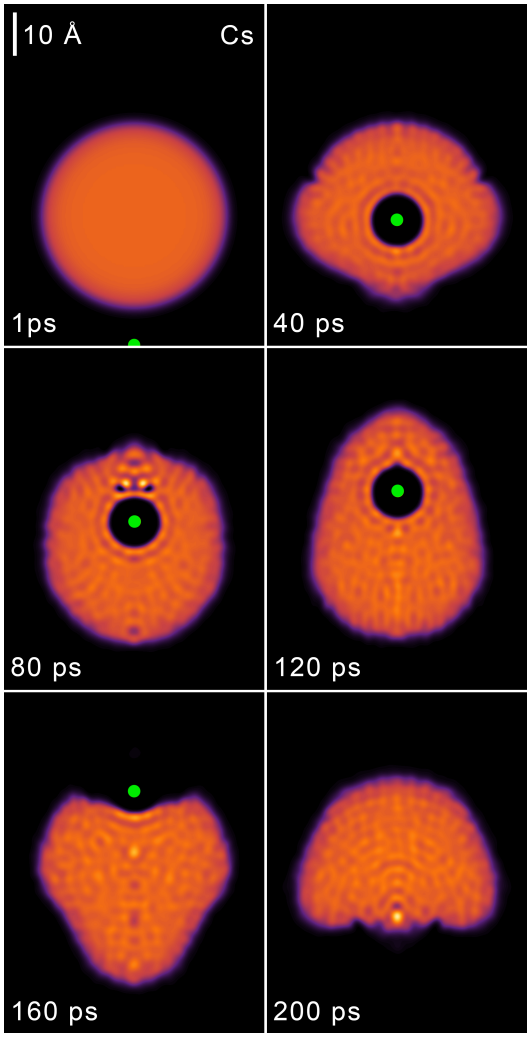

FIG. 5: Dynamic evolution of Cs (big dot) approaching from below the $N = 1000$ helium droplet at $v_{\mathrm{Cs}} = 200$ m/s and $b = 0$, going across it. The corresponding time is indicated in each frame. The two dark spots in the $t = 80$ ps frame are the cross section of a ring vortex about to collide with the atomic bubble approaching it from below.

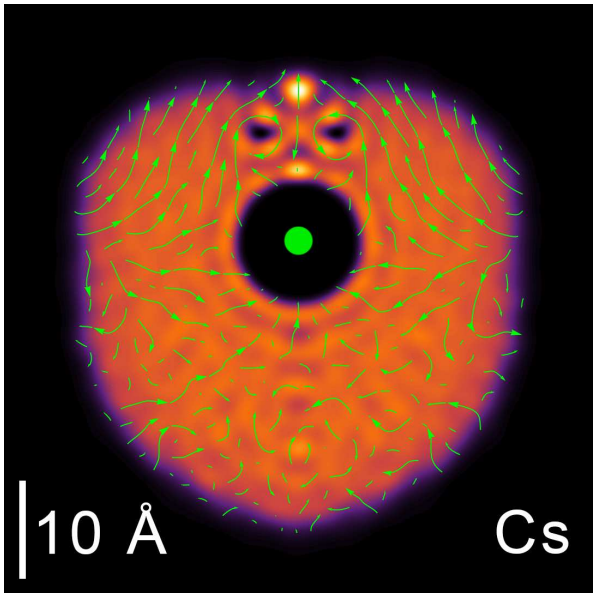

FIG. 6: Helium density at $t = 75$ ps showing a ring vortex approaching the Cs bubble from above. The circulation lines are represented in green. The situation corresponds to the head-on collision at $v_{\mathrm{Cs}} = 200$ m/s.

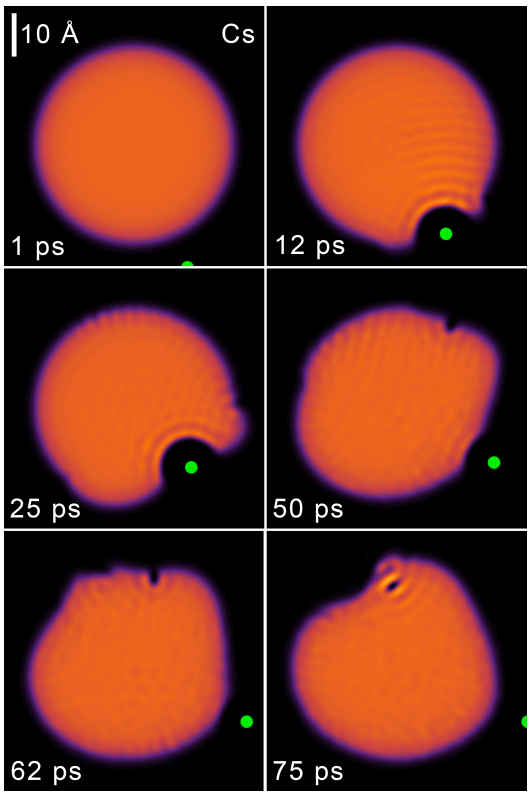

FIG. 7: Dynamic evolution of Cs (big dot) approaching from below the $N = 1000$ helium droplet at $v_{\mathrm{Cs}} = 100$ m/s and $b = 11$ Å. The corresponding time is indicated in each frame.

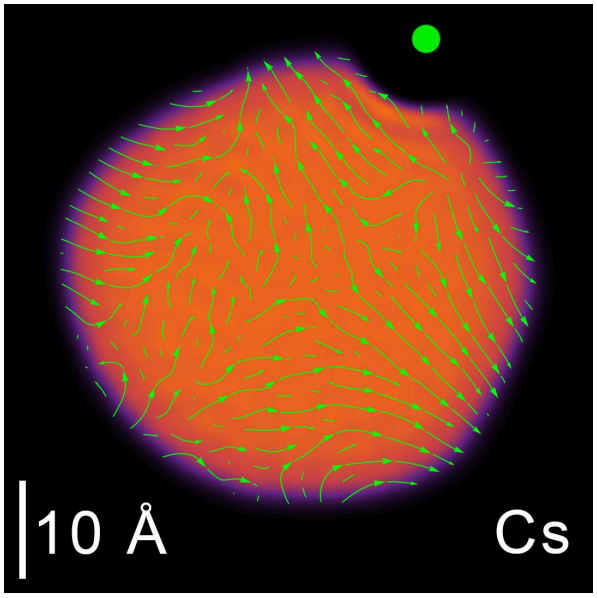

FIG. 8: Particle flow pattern at $t = 385$ ps corresponding to the $v_{\mathrm{Cs}} = 50$ m/s and $b = 11$ Å collision. The big dot represents the Cs atom.

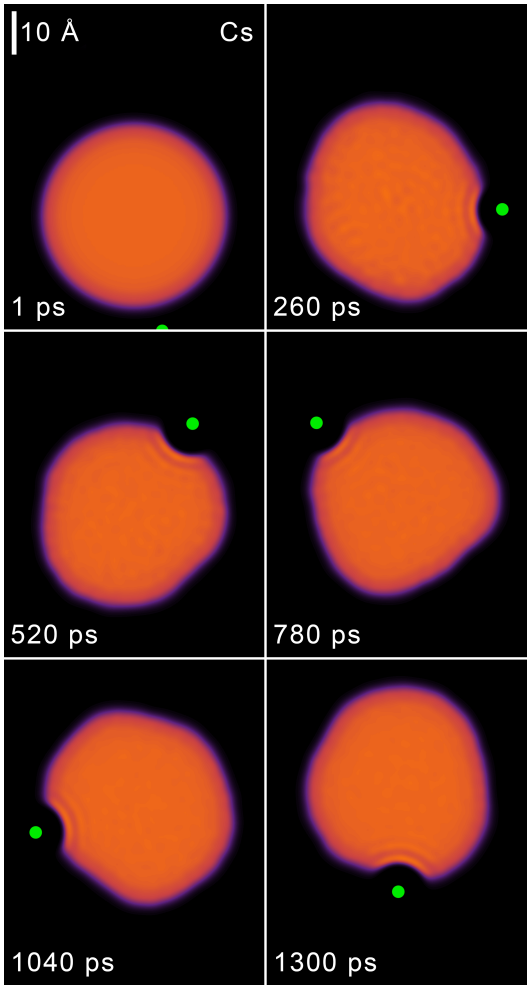

FIG. 9: Dynamic evolution of Cs (big dot) approaching from below the $N = 1000$ helium droplet at $v_{Cs} = 50$ m/s and $b = 9$ Å. The corresponding time is indicated in each frame.